PHILOSOPHICAL TRANSACTIONS OF THE ROYAL SOCIETY A MATHEMATICAL, PHYSICAL & ENGINEERING SCIENCES

The Adsorption of Krypton and Xenon on Evaporated Metal Films

D. Brennan and M. J. Graham

Phil. Trans. R. Soc. Lond. A 1965 **258**, 325-345
doi: 10.1098/rsta.1965.0044

THE ADSORPTION OF KRYPTON AND XENON ON EVAPORATED METAL FILMS

By D. BRENNAN and M. J. GRAHAM

Department of Inorganic, Physical and Industrial Chemistry, The University of Liverpool

(*Communicated by C. E. H. Bawn, F.R.S.—Received* 21 *July* 1964— *Read* 25 *February* 1965)

CONTENTS

The relative effective areas of krypton and xenon atoms adsorbed on iron, cobalt, nickel, titanium, zirconium, molybdenum, tungsten, tantalum and platinum have been examined by determination of the 77 °K isotherm for each gas adsorbed successively on the clean surface of the same evaporated film. Point *A*, point *B* and the B.E.T. equation have been used to assess the monolayer value, with the general result that the number of atoms required to complete the monolayer is the same for xenon as for krypton, despite the larger atomic size of xenon. This result is interpreted to mean that both kinds of atoms occupy the same sites and that their effective area is determined by the site area. The more usual supposition that adatoms are close-packed, each exerting a characteristic area independent of the nature of the surface, is rejected.

Various configurations of adatoms are examined with the object of finding the densest occupation of available sites. For this purpose, interatomic energies have been calculated using the Lennard-Jones (6:9) and (6:12) potentials and the Buckingham exp:6 potential. In several instances, clear decisions can be reached, and the general conclusion is that equal numbers of krypton and xenon atoms are required to form the monolayer, in keeping with experiments.

Introduction

Because of its inertness, adsorbed krypton has been used frequently to provide a parameter defining the surface area of metals. More recently, xenon has been used for the same purpose, it having the advantage of a much lower saturated vapour pressure than krypton at a given temperature, and so permits the use of a conventional adsorption apparatus to

Vol. 258. A. 1089. (Price £1. 3*s*.; U.S. $3.45) 41 [Published 11 November 1965

attain high relative pressures, at the temperature of boiling liquid nitrogen, without the need to apply large corrections for the dead volume. The aim of the present investigation was to compare the adsorptive capacity of a given surface for both krypton and xenon, under comparable conditions, and so throw light on the controversy concerning the effective areas of adsorbed krypton and xenon atoms (Brennan, Graham & Hayes 1963). At the same time, the investigation has given the opportunity for a reappraisal of the method of Brunauer, Emmett & Teller for evaluating monolayer coverages. It has also enabled the results of recent investigations with the field emission microscope to be correlated with results obtained by classical methods employing a different kind of surface.

Interest in surface area measurements has been sustained because a knowledge of the surface concentration of an adsorbate is often vital to the identification of the adsorbed species and the elucidation of its configuration. An examination of possible configurations of krypton and xenon on metals has been made, in the knowledge of the present results, with the main finding that, while surface concentrations and configurations are in general the same for the two substances, differences in surface concentrations between different crystallographic faces and between different metals may occur which can have important implications for the interpretation of chemisorption processes; this latter aspect is considered for the adsorption of carbon monoxide in the next paper.

Experimental

The adsorption apparatus was of classical design. Essentially, it comprised a cylindrical adsorption vessel (4·5 cm diameter, 20 cm length), a dosage volume and a storage volume, each isolated by stopcocks. Pumping was by a two stage mercury diffusion pump backed by a mechanical pump. Absolute pressure measurements were made by means of a McLeod gauge, having a 600 ml. bulb and a 1 mm bore capillary. An Alpert type ionization gauge was used to mesure pressures of xenon too low to be accessible with the McLeod gauge; the ion gauge was used also to monitor the vacuum. A Pirani gauge was used to determine when the adsorption of a dose of gas was complete. Heating tapes and ovens were used to achieve bakeout at about 450 °C of the apparatus as one piece, except for the stopcocks, which were water cooled and the tubulation of which could be heated to within 0·5 in. of the key (Brennan & Hayes 1962). In this way, vacua of the order of 10^{-8} torr could be attained after overnight bakeout of an aged apparatus. No stopcock communicated directly with the adsorption vessel except via a cold trap.

Films were deposited onto the glass at 0 °C by direct evaporation of hairpin filaments suspended from tungsten hooks, except for platinum and zirconium which were deposited indirectly from a tungsten filament. All the metals were thoroughly outgassed before deposition; sometimes a preliminary outgassing was given in a subsidiary apparatus and, with the metals of lower melting point, a period of several days was necessary to produce a clean sample. It has been suggested (Hickmott & Ehrlich 1958) that the surfaces of evaporated metal films may not be clean because of outgassing of the filament when the temperature is raised to the value for evaporation to occur. This will certainly happen if the preliminary outgassing has not been thorough, but we find, as does Roberts (1963), that with adequate outgassing just below the evaporation temperature, and if necessary at a temperature at which some evaporation does occur, it is possible to reduce volatile

impurities to a level at which no significant contamination of the film occurs during its deposition. All the films were sintered at 60 °C for 10 min. The metals were supplied by Johnson, Matthey & Co. Ltd and were of high purity; when available, spectroscopically standardized samples were used.

The useful range of the ionization gauge with respect to xenon extended only to about 3×10^{-4} torr, above which the ion current ceased to be proportional to pressure. However, this upper limit was just adequate to permit calibration of the gauge, by direct comparison with the McLeod gauge. The gauge factor was determined to an accuracy of 8% and had a value of 3·2 relative to the value for air.

The krypton and xenon used were supplied in break-seal ampoules by British Oxygen Gases Ltd. The purity of the krypton was 99 to 100% with xenon as the possible impurity. The xenon was found to contain a more volatile impurity which could be removed by repeated distillation from one liquid nitrogen cold trap to another, with pumping. Any given sample of the gas treated in this way on several occasions, and different samples, always yielded a constant vapour pressure having the value $2{\cdot}3 \times 10^{-3}$ torr at the temperature of boiling liquid nitrogen when corrected for thermal transpiration by the equation of Bennett & Tompkins (1957). This value is somewhat higher than that of $1{\cdot}7 \times 10^{-3}$ torr at 77 °K obtained by Podgurski & Davis (1961) from careful measurement, but the difference could be accounted for by an uncertainty in bath temperature of only 1 degC. Having in mind that our measurement did not enjoy all the precautions necessary for the determination of a highly accurate value for the saturated vapour pressure, we believe that the value obtained by us is sufficiently constant, reproducible and close to the accepted value to warrant the belief that the xenon used in this work was not significantly contaminated with impurity.

An adsorption isotherm was obtained by admission of successive increments of gas to the film; the size of each increment could be measured during the course of an experiment and so could be made bigger when it was desired to increase the pressure over the film more rapidly. Corrections for the dead volume were obtained by direct measurement in the absence of a film. In the calibration, no allowance was made for adsorption on the glass of the adsorption vessel which later would be covered by the film, since adsorption on glass at the very low relative pressure at which the point B occurs for the metals is negligible. Further, the surface areas of the films were generally very much greater than their geometrical areas so that significant error is not likely even at the higher relative pressures, except possibly for the low area metals, like platinum, and then to not more than 5%.

Results

Measurements at 77 °K

The specification of a temperature of 77 °K in this paper should be interpreted to mean 'the temperature of boiling liquid nitrogen at atmospheric pressure'. The procedure adopted for all the metals entailed the adsorption of xenon first, followed by its complete removal from the system by pumping. Krypton was then adsorbed and removed, and, finally, xenon was adsorbed again. For the purpose of speeding up the desorption of the gases, the film was brought to a temperature of −80 °C with a bath of solid carbon dioxide

in alcohol. The coincidence, or near coincidence, of the two xenon isotherms is an unequivocal criterion of an unchanging surface and bath temperature throughout the entire sequence of measurements.

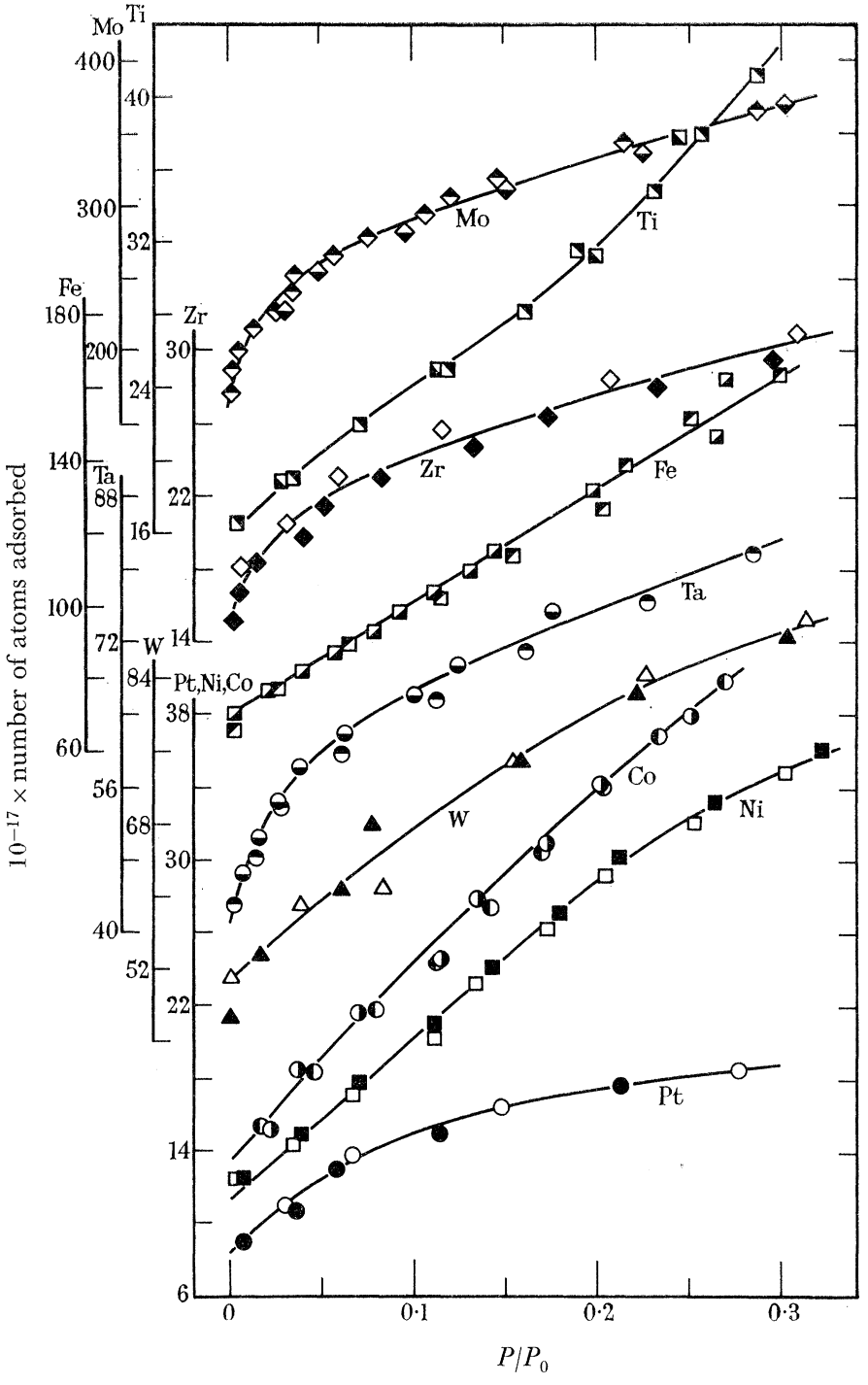

FIGURE 1. The 77 °K isotherms for the adsorption of xenon on evaporated films of platinum (35·1 mg), nickel (65·3 mg), cobalt (64·8 mg), tungsten (32·4 mg), tantalum (45·8 mg), iron (83·8 mg), zirconium (15·8 mg), titanium (35·3 mg) and molybdenum (77 mg); P_0 (xenon, 77 °K) = $2{\cdot}3 \times 10^{-3}$ torr. The points ○, □, ◐, △, ◒, ◪, ◇, ◩ and ◆ denote measurements made prior to the adsorption of krypton and the other points were obtained after krypton adsorption.

The xenon isotherms up to a relative pressure of about 0·3 are shown in figure 1 and again in figure 2, where the data are presented according to the B.E.T. equation. Some of the B.E.T. plots are fairly linear over this pressure range, but not necessarily with the same slope as at very low relative pressures. The krypton and xenon isotherms are compared in figure 3 which employs a more open pressure scale. For xenon, all the metals exhibit well defined points B; indeed, point A and point B are essentially the same in this case.

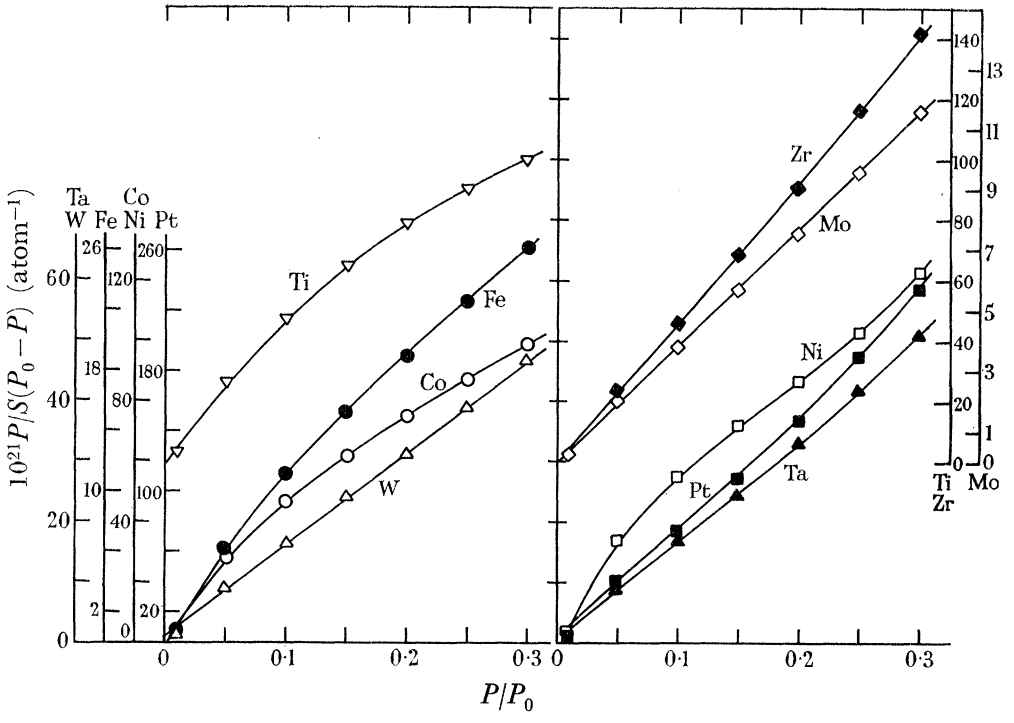

FIGURE 2. Isotherms in the region of high relative pressure for the adsorption of xenon on the metals, at 77 °K, plotted with reference to the equation of Brunauer, Emmett & Teller.

For krypton, many of the metals exhibit well defined points A and B, but not all. In table 1, the various criteria of monolayer capacity are assembled for comparison. All the metals show a capacity for adsorption of xenon beyond point B and in some cases this higher pressure adsorption is considerable.

TABLE 1. COMPARISON OF THE VARIOUS CRITERIA OF MONOLAYER COVERAGE (10^{17} ATOMS) FOR KRYPTON AND XENON ADSORBED ALTERNATELY ON THE SAME EVAPORATED FILM AT 77 °K

			point A		point B		B.E.T. equation			
metal	weight (mg)	type	Kr	Xe	Kr	Xe	Kr $\frac{P}{P_0} < 0{\cdot}02$	Xe $\frac{P}{P_0} < 0{\cdot}02$	Xe $\frac{P}{P_0} < 0{\cdot}04$	Xe $\frac{P}{P_0} > 0{\cdot}04$
Co	64·8	f.c.c.	11·6	13·9	12·4	13·9	14·1	16·2	17·3	—
Ni	65·3	f.c.c.	11·4	11·0	11·6	11·0	12·5	13·2	14·1	—
Pt	35·1	f.c.c.	7·4	8·5	8·2	8·5	10·2	10·7	11·8	14·1
Fe	83·8	b.c.c.	70	67	74	67	84	75	80	—
Mo	77·0	b.c.c.	[186]	[194]	[220]	[226]	241	226	234	260
Ta	45·8	b.c.c.	40	44	43	44	53	53	56	60
W	32·4	b.c.c.	50	51	53	51	56	56	56	67
Ti	35·3	h.c.p.	—	16·3	—	16·9	21·2	19·8	20·1	—
Zr	15·8	h.c.p.	—	—	—	20·8	23·2	22·3	22·6	22·6

Measurements at 111 °K

Because the heat of adsorption of xenon on the metals is greater than that of krypton (cf. table 2) point B, for the xenon isotherms will be found at lower relative pressures than for krypton at a given temperature. To test the effect of raising the temperature of the

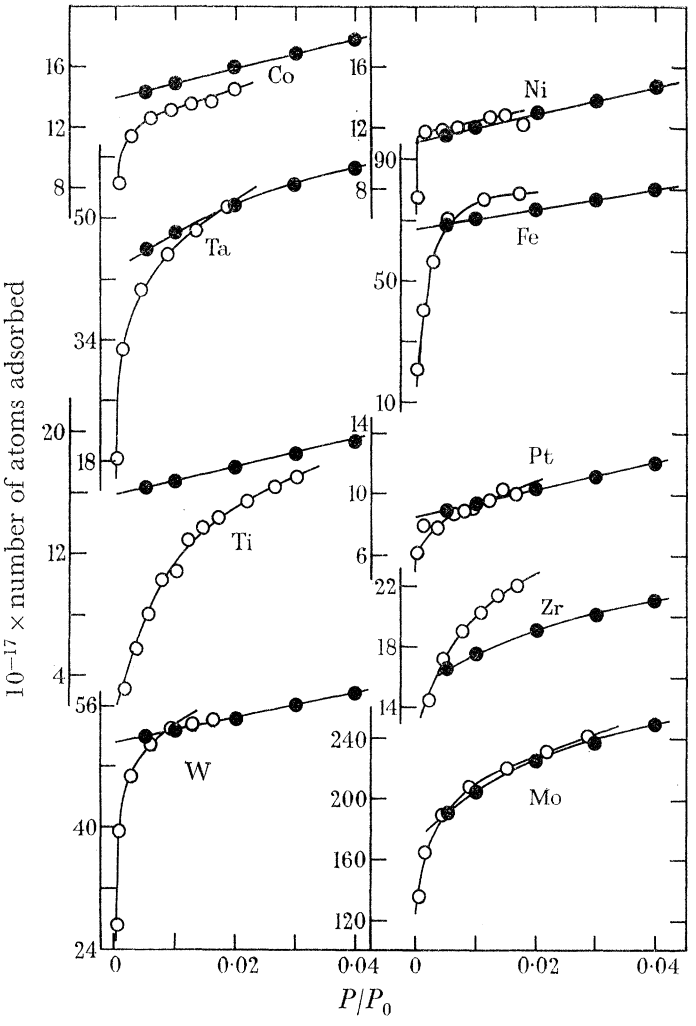

FIGURE 3. The 77 °K isotherms for the adsorption of krypton (○) and xenon (●) at low P/P_0, on evaporated films of tungsten, titanium, tantalum, cobalt, nickel, iron, platinum, zirconium and molybdenum; P_0 (krypton, 77 °K) = 3 torr. The surfaces are the same as those referred to in figure 1 from which the data for xenon have been obtained by interpolation.

xenon adsorption to a value which would make the ratio *heat of adsorption*: RT comparable to that for the krypton adsorption, measurements were made with xenon at the temperature of melting isopentane. Pure isopentane melts at 113 °K, but samples not subject to careful purification will generally have a lower melting point. A value of P_0 (xenon) = 3·8 torr was determined at the melting point of our material, corresponding to a temperature of 111 °K (Freeman & Halsey 1956). Thus, we conclude that neither the xenon nor the *iso*pentane used was seriously contaminated. Difficulties were encountered due to the high volatility and low latent heat of melting of isopentane. Measurements were

made with cobalt as the adsorbent and it is seen from figure 4 that the adsorption of xenon at the higher temperature is now somewhat less than that of krypton at 77 °K, whereas, when both adsorptions were carried out at 77 °K, the adsorption of xenon was slightly greater than that of krypton. It is interesting to note that both the curves of figure 4 exhibit similar curvature in the region of point *B*. In a film of this nature, there will be regions of imperfection on which the adsorbed atoms may not be so strongly held as on the main planes and these regions will be more favoured at 77 °K by xenon than by krypton because of the former's greater polarizability.

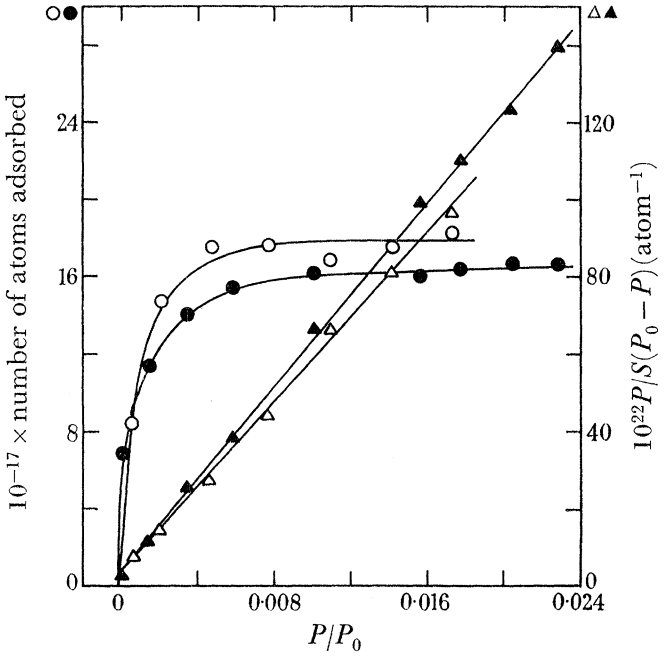

FIGURE 4. Isotherms and B.E.T. plots for the adsorption of xenon (●, ▲; 111 °K) and krypton (○, △; 77 °K) on a cobalt film (60 mg). P_0 (xenon, 111 °K = 3·8 torr. B.E.T. monolayer coverages: xenon, $16{\cdot}9 \times 10^{17}$; krypton, $18{\cdot}2 \times 10^{17}$ atoms.

DISCUSSION

Criteria of monolayer coverage

There is no one parameter that can be used unequivocably to define monolayer coverage. Point *A* and point *B* are intuitive quantities and the B.E.T. equation can no longer be given a higher status than that of an empirical relation, despite its original association with a model of the physisorbed state. There is still no certain way of deciding to what extent the first adsorbed layer is complete before multilayer adsorption becomes significant. It is fortunate that the isotherms for the adsorption of inert gases on metals often exhibit a very well defined point *B* (e.g. iron, cobalt and nickel) and, even in those cases (e.g. molybdenum and zirconium) where point *B* cannot be located with an accuracy good enough to permit its use in the assessment of monolayer coverage, there is still a very strong curvature of the isotherm in the vicinity of point *B*. Consequently, an expression of the form of the B.E.T. equation, or the Langmuir isotherm to which it closely approximates at the low values of P/P_0 involved, can be expected to yield a more definitive parameter related to monolayer coverage than either point *A* or point *B*. The question remains whether such a

parameter can be identified with the monolayer coverage. Thus, for example, Ross & Olivier (1961) have shown that a Langmuir type isotherm is a possible consequence of a model quite different from the Langmuir model and the monolayer coverage derived from the more sophisticated model may be different from that which would be obtained from an expression having an algebraic form similar to the Langmuir equation. However, it seems very reasonable to suppose that, where point *B* is as well defined as here, the monolayer capacity is to be found somewhere in its immediate vicinity and that there is no appreciable multilayer adsorption before the point *B*. Accordingly, it is felt that the estimates of the monolayer coverage provided for the systems by the Langmuir equation or the B.E.T. equation, applied to adsorption at low values of relative pressure, cannot be greatly in error. Inspection of table 1 shows that the use of the B.E.T. equation at relative pressures appreciably higher than correspond to the region of point *B* can give estimates of the monolayer coverage significantly different from those derived from data in the vicinity of point *B*. This is not very surprising because considerable adsorption occurs after point *B* and it is improbable that the adsorbed state corresponds to any model from which the B.E.T. equation is derivable. The fact that the B.E.T. equation can be fitted to the adsorption data under these circumstances for some metals need have no real significance and, indeed, for some metals (e.g. cobalt and titanium) such a fit is not possible. This point has been made by P. Cannon & Gaines (1961), but is stressed again here because assessments of monolayer coverage are often made by application of the B.E.T. equation to data well removed from point *B* and, with special reference to the estimation of the effective areas of adsorbed krypton and xenon atoms, the deductions of W. A. Cannon (1963) can be criticized on this score.

While it is valuable to have an absolute measure of the monolayer coverage, the question of the relative size of adsorbed krypton and xenon atoms can be settled much more directly. Reference to table 1 shows that similar criteria of monolayer coverage give very similar values for the number of krypton and xenon atoms adsorbed. For some of the metals the agreement is very good. For cobalt, where the agreement is not so good, more xenon than krypton atoms are to be found in the monolayer, despite their larger size; a similar result has been reported by Ponec & Knor (1962) for evaporated films of nickel. As already mentioned, this effect most likely arises in the greater heat of adsorption of xenon than of krypton (cf. table 2) enabling xenon to occupy sites too shallow to be occupied by krypton at the same temperature. The only significant discrepancy from the statement that the same number of krypton atoms as of xenon atoms are necessary to complete the monolayer is provided by iron for which the monolayer contains about 12% fewer xenon than krypton atoms and even this is less than the difference of 17% which would be expected if the atoms were close packed and exerted the same areas as they did in the solid state. However, the data of table 1, taken as a whole, provide strong justification for the conclusion that, in general, krypton and xenon atoms adsorbed on metals have the same effective cross-sectional area.

The equation of Dubinin & Radushkevich (1947) has been employed recently by Hobson (1961 *a*, *b*) to describe the isotherms of nitrogen, helium and argon on glass at low temperatures with a remarkable degree of self consistency. The equation has the form

$$\log_{10} S = \log_{10} S_m - D(\log_{10} P/P_0)^2,$$

where S is the number of molecules adsorbed and $D = AT^2$ is a constant; S_m is a constant which has been identified with the monolayer coverage. The equation was originally used to describe adsorption on porous media, but Hobson has pointed out that the excellence of its fit to his experimental data, obtained on a nonporous adsorbent and at relative pressures much below the region for which the equation was originally intended, must mean that it can now be regarded only as an empirical relation. In view of the impressive conformity of the relationship to Hobson's data, we have tested the isotherm in relation to the present data. Unfortunately, the S_m values derived are erratic because of the wide range of D values involved, particularly for krypton adsorption. It is concluded that the Dubinin–Radushkevich equation is unable to provide a useful criteria of the monolayer coverage for these systems.

Configuration of the adsorbed layer

It is a very difficult problem to calculate from first principles the surface configuration which would minimize the free energy. Rather, we will proceed in a somewhat intuitive manner with the aim of discovering descriptions of the surface state, which, while not rigorously established, do not seem objectionable and, at the same time, permit interpretations which support the arguments used by virtue of their self-consistency.

Site adsorption of inert gas atoms

The obvious deduction to be made from the finding that adsorbed krypton and xenon atoms have the same effective area is that these atoms occupy surface sites and that the number of atoms required to complete a monolayer is controlled by the density of sites. An attempt can be made to account, in like terms, for the widely different effective atomic areas obtained by Singleton & Halsey (1954) for xenon adsorbed on very different adsorbents (20·2 Å^2 on carbon black, 18·2 Å^2 on silver iodide and 27·3 Å^2 on anatase, relative to a value of 16·2 Å^2 for nitrogen), as discussed by Anderson & Baker (1962).

Confining our attention to inert gas-metal systems, there is good evidence from field emission microscopy (Ehrlich & Hudda 1959; Rootsaert, van Reijen & Sachtler 1962) to support the view that the adatoms are held on sites. The demonstration by this technique of the specificity of the adsorption on different crystallographic faces can be correlated with the coordination number of the site offered by a given plane. The better the adatom fits into the substrate structure, the more strongly it is held. The major part of the interaction energy arises by virtue of dispersion forces between the adatom and the metal atoms comprising the site which it occupies; the polarization energy does not account for more than about 20% of the total energy even though large surface potentials are observed for these systems (Ehrlich & Hudda 1959). This is a very different view of the adsorbed layer from that traditional in surface area assessment by measurement of adsorption where it is generally supposed that the adsorbate atoms or molecules exert a characteristic effective area and assume a close packed configuration, regardless of the surface involved.

A further argument in favour of site adsorption is to be found in the relatively high value of the activation energy required for diffusion of the adatom (cf. table 2). At the values of kT involved, it is clear that an atom on the surface moves by hopping from site to site and that it spends most of its time in occupation of a site.

PHILOSOPHICAL TRANSACTIONS OF THE ROYAL SOCIETY A MATHEMATICAL, PHYSICAL & ENGINEERING SCIENCES

TABLE 2. THE HEAT OF ADSORPTION AND THE ACTIVATION ENERGY FOR SURFACE DIFFUSION OF KRYPTON AND XENON ON METALS

metal	heat of adsorption (kcal/mole)	activation energy for diffusion (kcal/mole)
krypton		
Pt (Chon *et al.* 1962)	4·0	—
W (Ehrlich 1959)	4·5	1·0
xenon		
W (Ehrlich & Hudda 1959)	8–9	3·5
Mo (Ehrlich & Hudda 1961)	8	—
Ta (Ehrlich 1959)	5·3	—

In attempting to determine the monolayer capacity of different crystallographic faces, we will assume that sites are occupied to give the highest coverage compatible with only minor repulsion energies arising through interaction between neighbouring adatoms. To assess roughly the magnitude of the repulsion energy, if any, inherent in a given surface configuration, it is necessary to know the radius of the adatoms (R) and the form of the potential energy of interaction ($\mathscr{E}$) as a function of distance.

Diameter of adsorbed krypton and xenon atoms

We share the view of Sams, Constabaris & Halsey (1960) that, in the case of highly polarizable krypton and xenon, atomic size on the surface is best approximated to by atomic size in the solid state, because the force fields in the two cases are more likely to be similar than if comparison were made with the gaseous state.

The lattice constants of solid krypton and xenon have been determined by several groups of workers and their results are reviewed by Figgins & Smith (1960) for krypton, and Eatwell & Smith (1961) for xenon; there is a good measure of agreement between the results of the different investigations. (See also Sears & Klug 1962). We use the values $2R(\mathrm{Kr}) = 4{\cdot}06$ Å^2 and $2R(\mathrm{Xe}) = 4{\cdot}38$ Å^2.

Potential energy functions for the interaction between adatoms

In assessing the energy of interaction of adsorbed atoms for a given configuration, we will apply functions which have been derived from a study of three-dimensional phases and which are not therefore strictly applicable, to the two-dimensional adsorbed phase. Thus, the generation of a large surface potential by inert gas atoms adsorbed on metals arises by virtue of polarization of the adatom by the field associated with the electrical double layer at the metal surface (Ehrlich & Hudda 1959) and the unsymmetrical nature of the dispersion interaction with the metal (Sinanoğlu & Pitzer 1960) and there must, arise accordingly an additional repulsion energy not present in three dimensional phases. However, as the internuclear separation diminishes, the repulsion energy due to the interaction of electron clouds increases very much more rapidly than the energy due to repulsion between dipoles and, for appreciable overlaps, must be the dominant factor. This argument is probably an adequate justification for the neglect of electrostatic repulsion in a discussion which of necessity must be qualitative in character.

Three potential energy functions have been used frequently to describe interatomic interaction, but none can be regarded as more than an empirical relation because of the difficulty of accounting for repulsion energy; they are:

$$\text{(I)}\quad \mathscr{E} = \frac{a}{d^9} - \frac{b}{d^6},$$

$$\text{(II)}\quad \mathscr{E} = \frac{A}{d^{12}} - \frac{B}{d^6},$$

$$\text{(III)}\quad \mathscr{E} = \frac{\epsilon z}{z-6}\left\{\frac{6}{z}\exp z\left(\frac{d_0-d}{d_0}\right) - \left(\frac{d_0}{d}\right)^6\right\}.$$

I and II are the Lennard-Jones 6:9 and 6:12 potentials, respectively, and III is the Buckingham exponential:6 potential; d_0 in these expressions is the value of d, the internuclear separation, when the energy $\mathscr{E}$ is at a minimum. The 6:9 potential is often supposed to underestimate the repulsion energy, while the 6:12 potential almost certainly overestimates it; the exp:6 potential is sometimes regarded as a useful compromise. However, none of these functions is able with one set of coefficients to account for both transport and equilibrium properties and they have recently been vigorously criticized (McGlashan 1962). More successful in this respect is the power series of Guggenheim & McGlashan 1960*a*, *b*):

$$\text{(IV)}\quad \mathscr{E} = -\epsilon + \kappa\left(\frac{d-d_0}{d_0}\right)^2 - \alpha\left(\frac{d-d_0}{d_0}\right)^3 + \beta\left(\frac{d-d_0}{d_0}\right)^4,$$

but this expression is applicable only over a narrow range of d values. These expressions are compared in figure 5 and, for this purpose, the overlap of the van der Waals envelopes is defined by the parameter $\delta = d_0 - d$, with values of d_0 and the other coefficients best suited to the particular function as cited in the legend to the figure. It is to be noted that the function of Guggenheim & McGlashan is most similar to the 6:9 potential.

Criteria for the acceptability of a given configuration of adatoms

Surface configurations are built up by placing atoms on sites formed by metal atoms occupying positions in an undistorted lattice regardless of any differences in the sites involved, provided the coordination of the site is at least three. In doing this, the object is to achieve as high a concentration in the adsorbed layer as is compatible with an acceptable repulsive interaction between the adatoms calculated by means of the potential energy functions I, II and III. The heat of adsorption of xenon on metals is appreciably greater than that of krypton (table 2) and accordingly a somewhat larger repulsive energy can be tolerated in the case of xenon than krypton adsorption. For the purpose of calculating δ values for the various configurations, the values of R derived from the solid state, as given above, have been used and not the values derived from the potential energy functions; the corresponding values of $\mathscr{E}$ are then obtainable from the graphs of figure 6. An approximate estimate of the total energy of interaction (E) between adatoms has been obtained by summing $\mathscr{E}$ over near neighbours.

The crystal planes

Evaporated metal films will present a variety of crystal faces to the adsorbate and these must inevitably be somewhat imperfect. However, the low index planes will predominate

and, adhering to earlier arguments (Brennan, Hayward & Trapnell 1960), we will consider only the following planes: 100, 110 and 111 faces of the face-centred cubic metals; 100, 110 and 211 faces of the body-centred cubic metals; and 1000, 1100 and 1101 faces of the hexagonal close packed metals. The values for the radius of the metal atoms used in the calculations are those given by Pauling (1960).

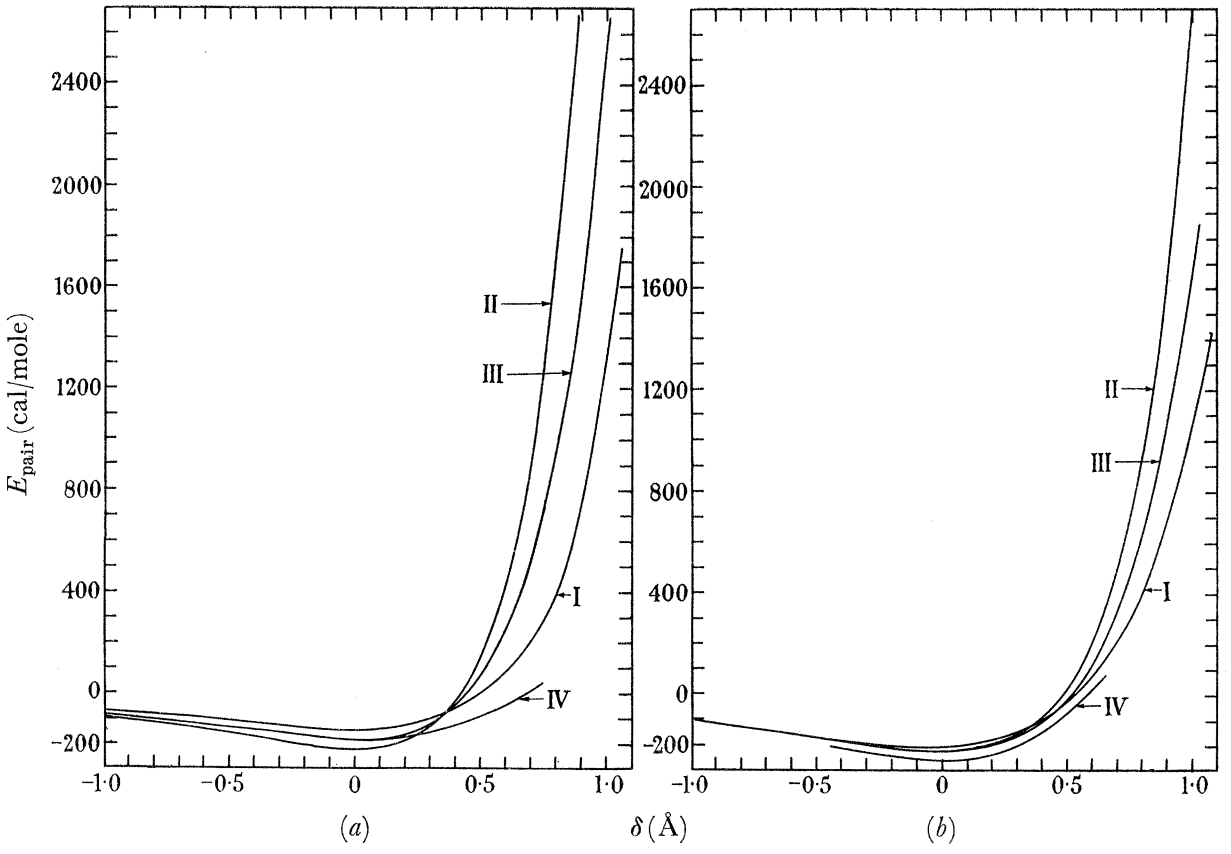

FIGURE 5. Potential energy functions for (*a*) krypton and (*b*) xenon; the numbers refer to krypton and xenon respectively.

(I) 6:9 *function*: $a = 10{\cdot}0 \times 10^7$, $33{\cdot}8 \times 10^7$ cal mole^{-1} Å^9; $b = 21{\cdot}6 \times 10^5$, $53{\cdot}4 \times 10^5$cal mole^{-1} Å^6 (Moelwyn-Hughes 1957).

(II) 6:12 *function*: $A = 30{\cdot}0 \times 10^8$, 140×10^8 cal mole^{-1}Å^{12}; $B = 16{\cdot}4 \times 10^5$, $35{\cdot}7 \times 10^5$ cal mole^{-1}Å^6 (Mason 1960).

(III) *exp*:6 *function*: $d_0 = 4{\cdot}036$, $4{\cdot}450$ Å, $\epsilon = 198{\cdot}8$, $229{\cdot}8$ cal/mole, $z = 13{\cdot}5$, $13{\cdot}0$ (Mason 1960).

(IV) *power series*: $d_0 = 4{\cdot}077$, $4{\cdot}438$ Å, $\epsilon = 190{\cdot}0$, $262{\cdot}8$ cal/mole, $\kappa = 6{\cdot}203 \times 10^3$, $8{\cdot}58 \times 10^3$ cal/mole, $\alpha = \beta = 2{\cdot}704 \times 10^4$, $3{\cdot}747 \times 10^4$ cal/mole (Guggenheim & McGlashan 1960*b*). The unit cal/mole here refers to the energy associated with one mole of atoms interacting as isolated pairs.

Hexagonal close packed metals

Titanium and zirconium are considered first because they permit clear conclusions to be reached more easily than do the other metals. These metals also exhibit strikingly different values (1·77 and 1·05, respectively) for the parameter $p = N(\mathrm{CO})/N(\mathrm{Kr})$, where $N(\mathrm{CO})$ is the number of molecules of carbon monoxide adsorbed at saturation and $N(\mathrm{Kr})$ is the

number of krypton atoms present in the monolayer on the clean surface. The present discussion has its clearest application in attributing these differences to differences in the values of N(Kr) for the two metals, rather than to differences in N(CO); this application is discussed in the next paper.

1000 *face*. This has a close packed configuration of metal atoms, as represented in figure 6, *A* and *B*. In this and similar figures, the circles serve merely to locate the centres of the species they represent, or their projection onto the plane of the paper; they are not drawn to scale. In configuration *A*, separation 1,2 is the critical one. Because of its very large lattice spacing, zirconium is able to adsorb krypton into this configuration without repulsion between atoms in the 1,2-positions (table 3). The smaller metallic radius of titanium gives rise to some repulsion between 1,2 adsorbed krypton atoms on this metal, but, even with the Lennard-Jones 6:12 potential, this is adequately offset by attractions between near neighbours in the 3- and 4-positions. Hence, for krypton adsorbed on both titanium and zirconium in configuration *A*, interactions between adatoms are, at worst, only mildly repulsive and it is concluded that this configuration is acceptable for these systems. Similarly, xenon can adsorb on zirconium in configuration (*A*). Xenon on titanium presents some difficulty. If potential II is used, there can be little doubt that the repulsions due to adatoms in the 1,2-positions are prohibitively large; but potential I and even potential III give rise to repulsions which might not be excessive, especially when it is remembered that reduction of repulsion would result if the adatoms moved slightly out of line and that the heat of adsorption of xenon is relatively large. It is concluded that xenon very likely adsorbs in configuration *A*, but, we note also that, if it cannot, then it will adopt configuration *B*, which is the next most densely packed arrangement and is free from repulsive interactions.

1100 *face*. In considering the 1100 plane (figure 6, *C* and *D*), it is necessary to consider also the metal atoms which occupy the plane which lies only $0{\cdot}577r$ below the surface and which, from the point of view of an adatom, must accordingly be considered to be part of the surface. An important consequence of the non-coplanarity of the metal atoms constituting an adsorption site is that the projections of their centres onto the 1100 plane will not be distributed symmetrically about the projection, onto the same plane, of the centre of the adatom occupying that site, with the result that adatoms may be brought closer together than they would were all the metal atoms coplanar. On the 1100 plane, the most dense configuration of atoms is *C* of figure 6 and, even for krypton on zirconium, the critical 1,2-separation of this configuration involves some repulsive interaction. However, for this particular case, the repulsion is more than offset by the attractive interaction with near neighbours and there is no doubt that krypton on zirconium can assume this configuration (cf. table 3). For xenon on zirconium in configuration *C*, the net interaction energy is very similar to that for xenon on titanium in configuration *A* and, as in that case, we suppose that configuration *C* is acceptable for xenon on zirconium, otherwise the alternative configuration *D* will be adopted. For krypton and xenon on titanium, configuration *C* involves prohibitively large repulsive interaction between adatoms, no matter which potential energy function is used, and the next most dense configuration *D*, for which all the interactions are attractive, will accordingly be adopted by these systems. Configuration *D* involves two kinds of site—one with co-ordination number three and the

PHILOSOPHICAL TRANSACTIONS OF THE ROYAL SOCIETY A MATHEMATICAL, PHYSICAL & ENGINEERING SCIENCES

TABLE 3 ADATOM OVERLAP DISTANCES (δ, Å) AND ESTIMATED TOTAL ENERGIES (E, CAL/MOLE) OF INTERACTION BETWEEN ADATOMS FOR THE VARIOUS CONFIGURATIONS DERIVED FROM (I) 6:9 FUNCTION, (II) 6:12 FUNCTION AND (III) exp:6 FUNCTION

The numbers in parentheses after the metals are the metallic radii (r, Å). The first two columns refer to the spacing involved and the number of neighbours at that spacing

hexagonal close packed metals (*figure* 6)

		Ti (1·46)								Zr (1·60)							
		E(Kr)				E(Xe)				E(Kr)				E(Xe)			
		δ	I	II	III	δ	I	II	III	δ	I	II	III	δ	I	II	III
								A, 1000 *plane*									
1, 2	2	0·64	260	1160	660	0·96	1700	4400	2760	0·32	−300	−240	−200	0·64	240	640	360
1, 3	2	−0·47	−220	−340	−320	−0·14	−400	−440	−440	−0·90	−160	−240	−180	−0·58	−320	−320	−320
1, 4	2	−1·06	−160	−180	−180	−0·74	−280	−280	−280	−1·55	−100	−100	−80	−1·23	−180	−180	−180
total energy			−120	640	160		1020	3680	2040		−560	−580	−460		−260	140	−140
								C, 1100 *plane*									
1, 2	2	0·92	1640	6200	3400	1·29	>6000	>10000	>8000	0·56	80	600	300	0·93	1500	3800	2400
1, 3	2	−0·61	−200	−300	−260	−0·42	−360	−360	−360	−0·95	−140	−220	−160	−0·73	−280	−280	−280
1, 4	2	−0·62	−200	−300	−260	−0·30	−380	−400	−400	−1·08	−160	−180	−160	−0·76	−280	−280	−280
total energy			1240	5600	2880		>5000	>9000	>7000		−220	200	−20		940	3240	1840
								E, 1101 *plane*									
1, 2	2	0·77	640	2900	1640	1·12	3200	>8000	>4000	0·44	−100	40	40	0·78	700	1700	1110
1, 3	1	−0·26	−140	−200	−190	0·01	−200	−230	−230	−0·60	−100	−50	−130	−0·34	−190	−200	−200
1, 4	2	−1·61	−100	−100	−100	−1·29	−180	−180	−180	−2·15	−60	−60	−60	−1·83	−120	−120	−120
total energy			400	2600	1350		2800	>7500	>3500		−260	−70	−150		390	1380	790

PHILOSOPHICAL TRANSACTIONS OF THE ROYAL SOCIETY A MATHEMATICAL, PHYSICAL & ENGINEERING SCIENCES

TABLE 3 (*cont.*)

face-centred cubic metals (*figure 7A*, 100 *plane*)

	Co, Ni(1·25)				Rh (1·35)				Pd (1·36)				Pt (1·39)			
	δ	I	II	III	δ	I	II	III	δ	I	II	III	δ	I	II	III
							krypton									
1, 2 4	0·53	80	840	400	0·24		attractive		0·22		attractive		0·13		attractive	
1, 3 4	−0·94	−320	−400	−360	−1·34		attractive		−1·38		attractive		−1·50		attractive	
total energy		−240	440	40			attractive				attractive				attractive	
							xenon									
1, 2 4	0·85	2080	5040	3480	0·56	120	480	200	0·54	40	360	120	0·45		attractive	
1, 3 4	−0·62	−600	−600	−600	−1·02	−320	−320	−320	−1·06	−320	−320	−320	−1·18		attractive	
total energy		1480	4440	2880		−200	160	−120		−280	40	−200			attractive	

body-centred cubic metals (*figure 8B*, 110 *plane*)

	Fe (1·24)				Mo (1·36)				W (1·37)				Nb, Ta (1·43)			
	δ	I	II	III	δ	I	II	III	δ	I	II	III	δ	I	II	III
							krypton									
1, 2 2	1·02	1840	>8000	5500	0·73	500	2240	1280	0·70	420	1800	1040	0·56	80	600	300
1, 3 2	0·01	−300	−440	−400	−0·39	−240	−380	−360	−0·42	−240	−360	−340	−0·62	−200	−150	−130
1, 4 2	−0·12	−300	−400	−400	−0·52	−220	−340	−300	−0·56	−200	−320	−280	0·72	−180	−200	−200
total energy		1240	>7000	4700		40	1520	620		−20	1120	420		−300	190	−30
							xenon									
1, 2 2	1·34	>5000	>8000	>6000	1·05	2520	>6000	>4000	1·02	2240	6000	3600	0·88	1200	2940	1920
1, 3 2	0·33	−220	−300	−300	−0·06	−400	−460	−460	−0·10	−400	−400	−440	−0·30	−380	−400	−400
1, 4 2	0·20	−360	−400	−400	−0·20	−400	−440	−440	−0·24	−400	−420	−420	−0·44	−360	−360	−360
total energy		>4000	>7000	>5000		1720	>5000	>3000		1440	5140	2740		460	2280	1160

other with coordination number four. In the site of co-ordination number four, an adatom just fails to contact the two lower metal atoms, but, despite this, it is unlikely that the adatom will move to one side in order to make contact with three metal atoms,

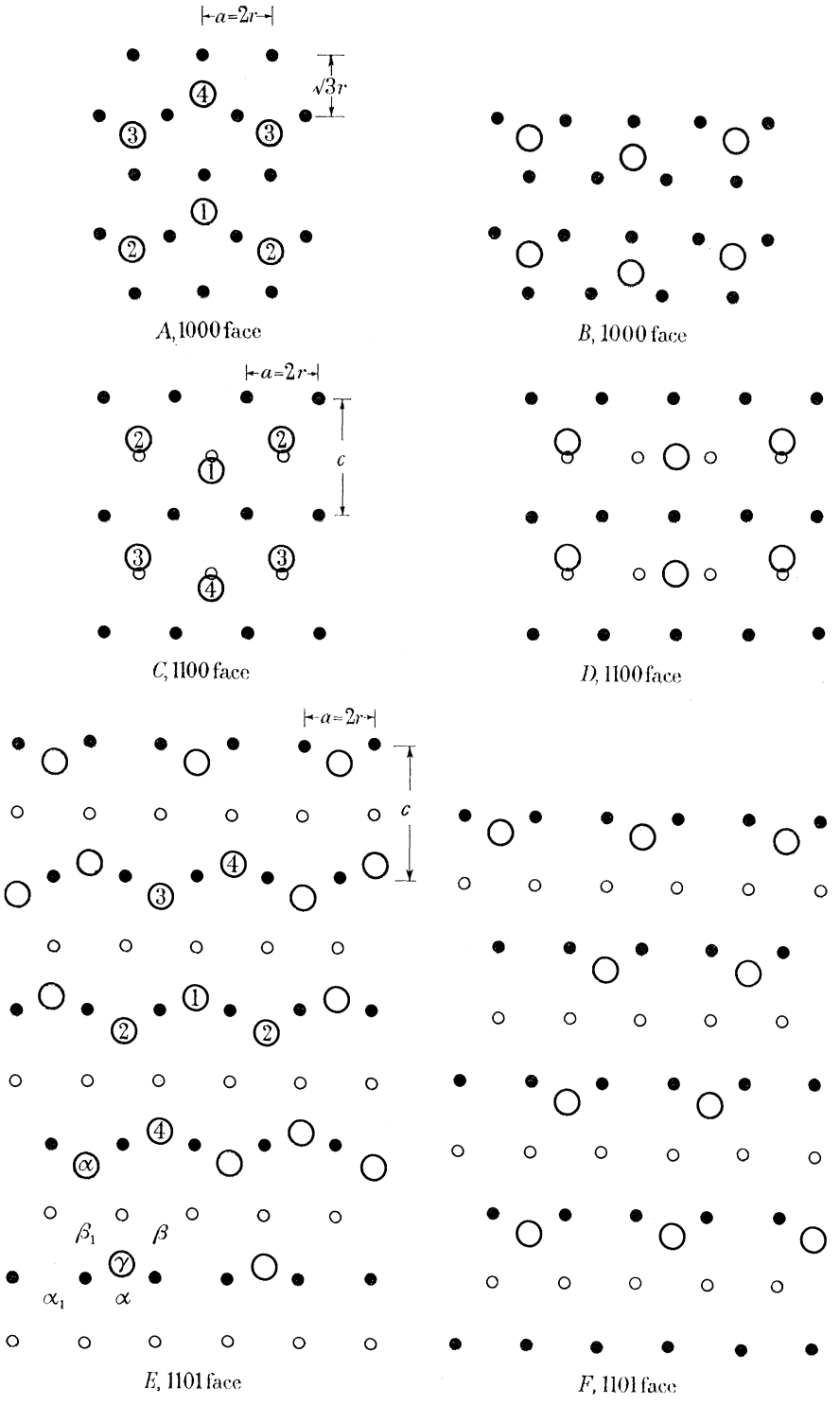

FIGURE 6. Adatom configurations for the hexagonal close packed metals. ●, The centres of metal atoms in the plane; ○, the centres of metal atoms 0·577r below the 1100 plane or 0·255r above the 1101 plane. O, the centres of adsorbed inert gas atoms.

PHILOSOPHICAL TRANSACTIONS OF THE ROYAL SOCIETY A MATHEMATICAL, PHYSICAL & ENGINEERING SCIENCES

preferring instead to experience a symmetrical interaction of slightly reduced energy with all four metal atoms as indicated in figure 6*D*.

1101 *face*. The surface of the 1101 plane will be considered to include those atoms which occupy the plane only $0{\cdot}255r$ above the 1101 plane proper (figure 6, *E* and *F*). This surface presents three types of sites to the adatom. An α site comprises two metal atoms in the 1101 plane and two metal atoms immediately above this plane. β and γ sites have a co-ordination number of three and differ in that the former has two metal atoms above the 1101 plane, while the latter has two in the 1101 plane (figure 6*E*).

Configuration *E* is the most dense that can be achieved on this plane because the repulsion between atoms occupying α_1 β_1 sites is prohibitively large. It is clearly permissible for krypton and xenon on zirconium, no matter which potential energy function is used and it is equally clearly not permissible for krypton and xenon on titanium (cf. table 3). The next most dense configuration is figure 6*F* in which the close approach α, γ is absent and for which the interaction energy is now entirely attractive.

TABLE 4. SURFACE COVERAGES FOR THE VARIOUS CONFIGURATIONS

For the hexagonal close packed metals, $a = 2r$ and $c = 4\sqrt{2}r/\sqrt{3}$; for the face-centred cubic metals, $a = 2\sqrt{2}r$; and for the body-centred cubic metals, $a = 4r/\sqrt{3}$

configuration	monolayer value (atoms per unit area)	applicability
	hexagonal close packed metals (*figure* 6)	
A, 1000 plane	$1/\sqrt{3}a^2$	Kr/Ti, Zr and Xe/Zr; probably Xe/Ti
B, 1000 plane	$2/3\sqrt{3}a^2$	alternative to *A* for Xe/Ti
C, 1100 plane	$1/ac$	Kr/Zr; probably Xe/Zr
D, 1100 plane	$2/3ac$	Kr, Xe/Ti; alternative for Xe/Zr
E, 1101 plane	$2/a\sqrt{(3a^2+4c^2)}$	Kr, Xe/Zr
F, 1101 plane	$1/a\sqrt{3a^2+4c^2}$	Kr, Xe/Ti
	face-centred cubic metals (*figure* 7)	
A, 100 plane	$1/a^2$	Kr, Xe/Rh, Pt; Kr/Co, Ni; probably Xe/Co, Ni
B, 110 plane	$1/\sqrt{2}a^2$	Kr, Xe/all the metals
C, 111 plane	$4/3\sqrt{3}a^2$	Kr, Xe/all the metals
	body-centred cubic metals (*figure* 8)	
A, 100 plane	$1/2a^2$	Kr, Xe/all the metals
B, 110 plane	$1/\sqrt{2}a^2$	Kr, Xe/Nb, Ta; Kr/Mo, W; perhaps Xe/Mo, W
C, 110 plane	$\sqrt{2}/3a^2$	Kr, Xe/Fe; alternative for Xe/Mo, W
D, 211 plane	$1/\sqrt{6}a^2$	Kr, Xe/all the metals

Conclusions for the hexagonal close packed metals. For the 1101 plane, it is expected that each metal will adsorb the same number of xenon as krypton atoms, but that the adsorptive capacity of zirconium should be twice that of titanium. The same is almost certainly true of the 1100 face, except that the ratio of adsorptive capacity of zirconium to that of titanium is 1·5. There is a doubt that fewer xenon atoms than krypton atoms will be adsorbed on the 1000 plane of titanium and the 1100 plane of zirconium, but there is a reasonable case that this not so. These conclusions are summarized in table 4. Reference to table 1 shows that the numbers of xenon and krypton atoms adsorbed on titanium and zirconium are very similar, which is in keeping with these expectations.

Face-centred cubic metals

Rhodium and palladium, although not the subject of adsorption studies with krypton and xenon, are included in this discussion because use will be made of these considerations when the adsorption of carbon monoxide is dealt with in the following paper.

100 *face*. Any attempt to achieve a configuration denser than that of figure 7 *A* would result in very large repulsive interactions between adatoms. For configuration *A*, the only system in this group which does not show a net attractive interaction is that of xenon on cobalt and nickel, for which the repulsive interaction is about the same as that considered acceptable for figure 6, *A* and *C*, with reference to xenon on titanium and zirconium, respectively. Accordingly, we believe that xenon is probably adsorbed in this configuration on cobalt and nickel, but, at the same time, we note that if this opinion is in error, then the next most dense configuration would be only half that for configuration *A*, figure 7 (cf. table 4).

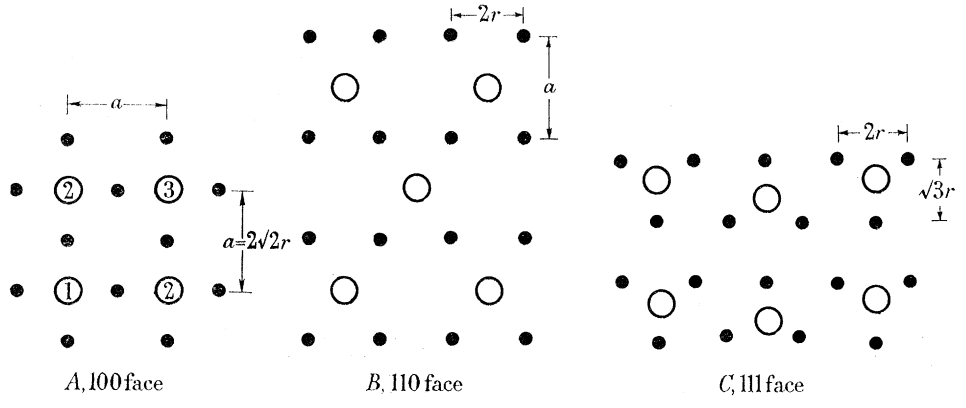

FIGURE 7. Adatom configurations for the face-centred cubic metals. ●, The centres of metal atoms in the plane; ○, the centres of adsorbed inert gas atoms.

110 *and* 111 *faces*. Configurations *B* and *C*, figure 7, referring to the 110 and 111 faces, respectively, are quite free from objection; attempts to achieve a closer packing of adatoms on sites lead to very large repulsive interactions.

Conclusions for the face-centred cubic metals. Apart from the case of xenon on the 100 plane of cobalt and nickel, all the faces of these metals have the same monolayer capacity for both krypton and xeonon, and even for the 100 face of cobalt and nickel, it is a reasonable assumption that the adsorption of both krypton and xenon involve the same sites. Thus, the requirements of this view of the adsorbed state are in keeping with the experimental findings set out in table 1.

Body-centred cubic metals

Again, reference will be made to a metal, namely niobium, not included in this study, because of its relevance to the following paper.

100 *and* 211 *faces*. Configurations *A* and *D*, figure 8, involve only attractive interactions between adatoms and are acceptable without qualification; the associated monolayer values are given in table 4.

110 *plane*. The closest spacing, namely the 1,2-separation of figure 8 *B*, involves repulsive interactions for both krypton and xenon on all the metals of this group (cf. table 3). For both krypton and xenon on niobium and tantalum, there is no doubt that the attractive interaction of near neighbours 1,3- and 1,4-spacings are adequate to offset the repulsive 1,2-interaction and, therefore, that configuration *B* is acceptable for these systems.

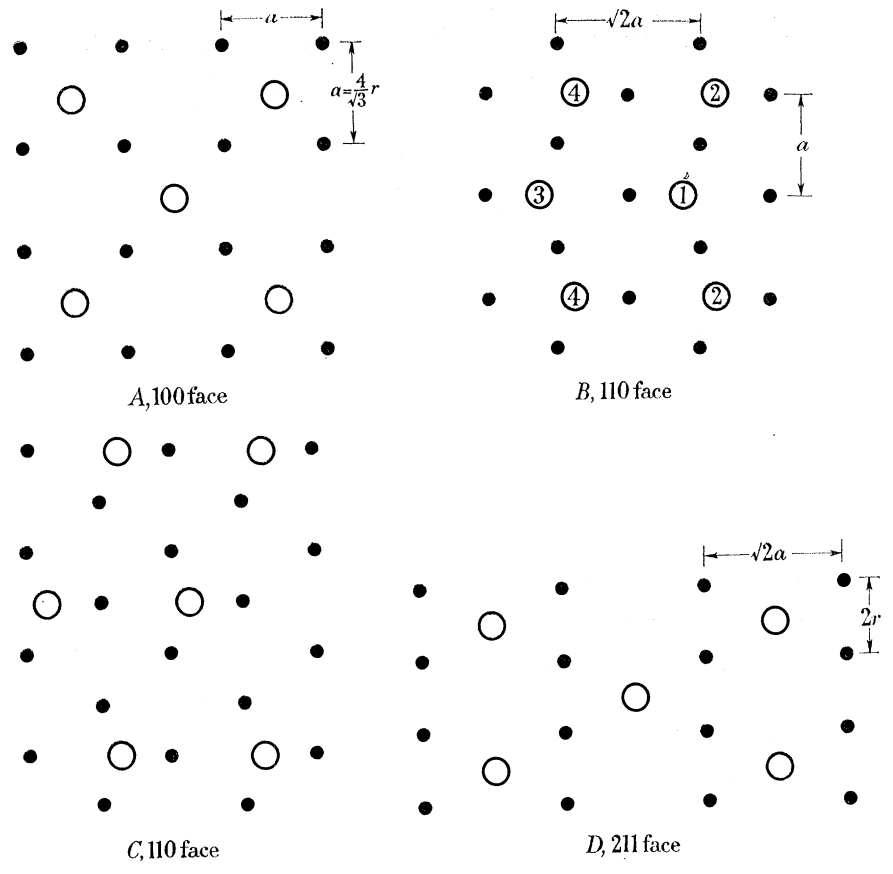

FIGURE 8. Adatom configurations for the body-centred cubic metals. ●, The centres of metal atoms in the plane; ○, the centres of adsorbed inert gas atoms.

Equally, there can be no doubt that, for both krypton and xenon on iron, the repulsive interaction due to nearest neighbour interaction cannot be adequately compensated for by attractive interaction with other neighbours and that, for this metal, configuration *B* is not feasible. In the case of iron, krypton and xenon will both assume configuration *C*, the next most densely packed arrangement, for which the energy of interaction between adatoms is entirely attractive. For molybdenum and tungsten, the position is not so clear. Krypton on molybdenum and tungsten in configuration *B* is very probably feasible if potential II does in fact over-emphasize the repulsive term of the interaction energy. Xenon on molybdenum and tungsten in configuration *B* will involve an even larger repulsive interaction and it is debatable whether configuration *B* is feasible for these systems. However, again having in mind the large heat of adsorption of xenon and the possibility of decreasing repulsive interaction by slight displacement of an adatom from the centre of an adsorption site, we consider that configuration *B* could well be adopted by

xenon on these two metals; it is also conceded that configuration *C* must be entertained as an alternative.

Conclusions for the body-centred cubic metals. The adsorption sites of the 100 and 211 faces do not distinguish between krypton and xenon in any case. For the 110 plane, niobium and tantalum adsorb equal numbers of krypton and xenon, but for molybdenum and tungsten there is a possibility that 1·5 times more krypton than xenon atoms could be adsorbed on this plane, although this possibility is not a strong one and the configuration on this plane of molybdenum and tungsten is probably the same as for niobium and tantalum. For the 100 plane of iron, it is also true that equal numbers of krypton and xenon atoms are adsorbed, but their configuration is different from that adopted on this plane of the other metals. The experimental finding (table 1) that these metals, apart from iron, adsorb very similar numbers of krypton and xenon atoms per unit area can thus be readily accommodated in terms of the proposed configurations. A given area of iron adsorbs about 12% more krypton than xenon atoms, but there is no way of achieving a higher density of krypton than xenon coverage in terms of these configurations. Reference is made again in the following paper, to the difficulties presented by the body-centred cubic metals.

Adsorption of xenon after point B

The coverage after point *B*, as revealed in figure 1, is attributable to some form of multilayer adsorption. The site distribution in the first layer is sufficiently open in some cases to permit appreciable interaction of a second layer adatom with the metal as well as with first layer adatoms. Consequently, it seems probable that a major part of the adsorption immediately after point *B* is occurring on sites formed by the adatoms of the first layer and the underlying metal atoms. The energy of adsorption of the second layer will be much smaller than that of the first layer, and although appreciably greater than that of the third and higher layers, the problem of estimating the coverage after point *B* is too difficult to be treated by the methods applied in this paper to the first layer.

The authors are grateful to the Department of Scientific and Industrial Research for a grant to one of them (M.J.G.)

References

Anderson, J. R. & Baker, B. G. 1962 *J. Phys. Chem.* **66**, 482.
Bennett, M. J. & Tompkins, F. C. 1957 *Trans. Faraday Soc.* **53**, 185.
Brennan, D., Graham, M. J. & Hayes, F. H. 1963 *Nature, Lond.* **199**, 1152.
Brennan, D. & Hayes, F. H. 1962 *J. Sci. Instrum.* **39**, 534.
Brennan, D., Hayward, D. O. & Trapnell, B. M. W. 1960 *Proc. Roy. Soc.* A, **256**, 81.
Cannon, P. & Gaines, G. L. Jr. 1961 *Nature, Lond.* **190**, 340.
Cannon, W. A. 1963 *Nature, Lond.* **197**, 1000.
Chon, H., Fisher, R. A., McCannon, R. D. & Aston, J. G. 1962 *J. Chem. Phys.* **36**, 1378.
Dubinin, M. M. & Radushkevich, L. V. 1947 *Proc. Acad. Sci. U.S.S.R.* **55**, 331.
Eatwell, A. J. & Smith, B. L. 1961 *Phil. Mag.* **6**, 461.
Ehrlich, G. 1959 *Structure and properties of thin films.* p. 423. Edited by Neugebauer, C. A., Newkirk, J. B. and Vermilyea, D. A. New York and London: Wiley.
Ehrlich, G. & Hudda, F. G. 1959 *J. Chem. Phys.* **30**, 493.

Ehrlich, G. & Hudda, F. G. 1961 *Res. Rep. No.* 61-RL-2828*M* by Ehrlich G., p. 3. Schenectady: General Electric Co.
Figgins, B. F. & Smith, B. L. 1960 *Phil. Mag.* **5**, 186.
Freeman, M. P. & Halsey, G. D. Jr. 1956 *J. Phys. Chem.* **60**, 1119.
Guggenheim, E. A. & McGlashan, M. L. 1960*a* *Proc. Roy. Soc.* A, **255**, 456.
Guggenheim, E. A. & McGlashan, M. L. 1960*b* *Mol. Phys.* **3**, 563.
Hickmott, T. W. & Ehrlich, G. 1958 *J. Phys. Chem. Solids*, **5**, 47.
Hobson, J. P. 1961*a* *J. Chem. Phys.* **34**, 1850.
Hobson, J. P. 1961*b* *Trans. 2nd Int. Vacuum Congr.* p. 146.
McGlashan, M. L. 1962 *Ann. Rep. Chem. Soc.* **59**, 88.
Mason, E. A. 1960 *J. Chem. Phys.* **32**, 1832.
Moelwyn-Hughes, E. A. 1957 *Physical chemistry*, p. 328. London, New York and Paris: Pergamon Press.
Pauling, L. 1960 *The nature of the chemical bond*, 3rd Edn. New York: Cornell Univ. Press.
Podgurski, H. H. & Davis, F. N. 1961 *J. Phys. Chem.* **63**, 1343.
Ponec, V. & Knor, Z. 1962 *Coll. Czech. Chem. Comm.* **27**, 1091.
Roberts, M. W. 1963 *Trans. Faraday Soc.* **59**, 698.
Rootsaert, W. J. M., van Reijen, L. L. & Sachtler, W. M. H. 1962 *J. Catalysis*, **1**, 416.
Ross, S. & Olivier, J. P. 1961 *J. Phys. Chem.* **65**, 608.
Sams, Jr., J. R., Constabaris, B. & Halsey, Jr., G. D. 1960 *J. Chem. Phys.* **64**, 1689.
Sears, D. R. & Klug, H. P. 1962 *J. Chem. Phys.* **37**, 3002.
Singleton, J. H. & Halsey, Jr., G. D. 1954 *J. Phys. Chem.* **58**, 330.
Sinanoğlu, O. & Pitzer, K. S. 1960 *J. Chem. Phys.* **32**, 1279.

PHILOSOPHICAL TRANSACTIONS OF THE ROYAL SOCIETY A MATHEMATICAL, PHYSICAL & ENGINEERING SCIENCES